HHS Public Access

Author manuscript

Hepatology. Author manuscript; available in PMC 2017 April 01.

Published in final edited form as:

Hepatology. 2016 April ; 63(4): 1213–1226. doi:10.1002/hep.28411.

Aspartate β-hydroxylase modulates cellular senescence via glycogen synthase kinase 3β in hepatocellular carcinoma

Yoshifumi Iwagami[1,*], **Chiung-Kuei Huang**[1,*], **Mark J. Olsen**[2], **John-Michael Thomas**[2], **Grace Jang**[2], **Miran Kim**[1], **Qiushi Lin**[4], **Rolf I. Carlson**[1], **Carl E. Wagner**[3], **Xiaoqun Dong**[4], and **Jack R. Wands**[1,#]

[1]Division of Gastroenterology & Liver Research Center, Warren Alpert Medical School of Brown University and Rhode Island Hospital, Providence, RI 02903

[2]Department of Medical Chemistry, College of Pharmacy Glendale, Midwestern University, Glendale, Arizona 85308

[3]Arizona State University, Glendale, Arizona 85306

[4]Department of Internal Medicine, College of Medicine, The University of Oklahoma Health Sciences Center, Oklahoma City, OK 73104

Abstract

Background & Aims—Aspartate β-hydroxylase (ASPH) is an enzyme overexpressed in human hepatocellular carcinoma (HCC) tumors and participates in the malignant transformation process. We determined if ASPH was a therapeutic target by exerting effects on cellular senescence to retard HCC progression.

Methods—ASPH knockdown or knockout was achieved by shRNAs or CRISPR/Cas9 system, respectively, whereas enzymatic inhibition was rendered by a potent 2nd generation small molecule inhibitor (SMI) of ASPH. Alterations of cell proliferation, colony formation and cellular senescence were evaluated in human HCC cell lines. The potential mechanisms for activating cellular senescence were explored using murine subcutaneous and orthotopic xenograft models.

Results—Inhibition of ASPH expression and enzymatic activity significantly reduced cell proliferation and colony formation, but induced tumor cell senescence. Following inhibition of ASPH activity, phosphorylation of GSK3β and p16 expression were increased to promote senescence whereas cyclin D1 and PCNA were decreased to reduce cell proliferation. The mechanisms involved demonstrate that ASPH binds to GSK3β and inhibits its subsequent interactions with AKT and p38 upstream kinases as shown by co-immunoprecipitation. *In vivo* experiments demonstrated that the SMI treatment of HCC bearing mice resulted in significant dose-dependent reduced tumor growth, induced phosphorylation of GSK3β, enhanced p16 expression in tumor cells and promoted cellular senescence.

[#]**Correspondence to:** Jack R. Wands, M.D., Liver Research Center, Rhode Island Hospital and The Warren Alpert Medical School of Brown University, 55 Claverick Street, 4th Fl., Providence, RI 02903. Jack_Wands_MD@Brown.edu; Tel: 401-444-2795; Fax: 401-444-2939.

[*]These authors contributed equally to this work.

Disclosures: The authors disclose no conflict of interest.

Conclusions—We have identified a new mechanism that promotes HCC growth and progression by modulating senescence of tumor cells. These findings suggest that ASPH enzymatic activity is a novel therapeutic target for HCC.

Keywords

ASPH; small molecule inhibitor (SMI); p16; CRISPR/Cas9

Introduction

Hepatocellular carcinoma (HCC) is the fifth most common tumor and the third leading cause of cancer mortality worldwide. (1) During the past two decades, the incidence of HCC has tripled whereas its 5-year survival rate has remained <12%. (2) Successful surgical resection helps to improve the overall survival; however, >80% of HCC tumors are unresectable at diagnosis and there are very limited therapeutic options for those patients. (3) Therefore, it is essential to explore the molecular mechanisms of HCC growth and progression in order to identify new targets for therapy.

Aspartate β-hydroxylase (ASPH) is a ~86-kDa type II transmembrane protein that belongs to the α-ketoglutarate-dependent dioxygenase family. (4) ASPH catalyzes the hydroxylation of aspartyl and asparaginyl residues in the epidermal growth factor (EGF)-like repeats in a variety of proteins, such as Notch receptors and ligands. (5) It was originally described as overexpressed in HCC and cholangiocellular carcinoma (CCC). (6) Currently, ASPH has been found upregulated in more than 20 tumor types, such as HCC, CCC, pancreatic, colon, breast and non-small cell lung cancer. (7–11) Interestingly, ASPH is overexpressed in 85–90% of human HCC, but not in dysplastic nodules and normal liver (7); it is rarely expressed in normal adult tissues except the placenta. (6) These findings support the hypothesis that ASPH is a necessary component for transformation of normal cells to a malignant phenotype. (12) Moreover, ASPH can be considered as a potential therapeutic target since it is expressed on the tumor cell surface where the catalytic site in the C-terminal region may be available for drug targeting. Recently, we have demonstrated that small molecule inhibitors (SMIs) of ASPH, which fit into the pocket of the catalytic site and inhibit enzymatic activity, produce anti-tumor effects in HCC and pancreatic ductal adenocarcinoma. (7, 8) The biologic activity of SMIs was partially mediated through inhibition of Notch signaling. (7, 8) However, there may be other biologic functions of ASPH, when overexpressed, that contribute to the generation of malignant phenotypes.

Cellular senescence is a phenomenon that normal cells have a limited ability to proliferate in culture. (13) The senescent phenotype may be induced by multiple stimuli, such as telomere shortening, chromosomal perturbation, oxidative damage and activation of oncogenes. (14) Some of these senescence-inducing stimuli are potentially oncogenic. During malignant transformation, tumor cells will acquire mutations that allow them to bypass and avoid senescence. (15) Thus, cellular senescence is considered to be a potent tumor-suppressor mechanism, which blocks incipient cancer cells from proliferating. (16, 17)

Inhibition of ASPH expression and activity may be a therapeutic intervention by guiding HCC cells to senescence. In this study, it was observed that shRNAs-mediated knockdown

and CRISPR/Cas9-mediated knockout as well as enzymatic inhibition of ASPH successfully trapped human HCC cells into senescence. It was further revealed that inhibition of ASPH activity induced cellular senescence through phosphorylation of the glycogen synthase kinase 3β (GSK3β). Mechanistically, ASPH inhibits phosphorylation of GSK3β through direct binding to GSK3β and blocking the action of its upstream kinases and downstream targets.

Experimental Procedures

Characterization of SMIs for ASPH

We developed, characterized and evaluated novel SMIs for ASPH β-hydroxylase activity as described previously. (7, 8) Based on the crystal structure of the ASPH catalytic site, computer generated drug design was performed, leading to the synthesis of a series of parent compounds and derivatives likely to fit into the pocket of the catalytic site and inhibit its enzymatic activity. The compound MO-I-1151 is a 2nd generation SMI chosen for study. It has been characterized by the following features compared to a first generation SMI (MO-I-1100) (7, 8): in that it 1) is more soluble; 2) has higher binding affinity to the ASPH catalytic site; and 3) exhibits an enhanced inhibitory effect on β-hydroxylase activity. (7)

Cellular Proliferation Assay

The cellular proliferation rate was measured using the 3-(4,5-dimethylthiazol-2-yl)-2,5-diphenyl-tetrazolium bromide (MTT; Sigma-Aldrich, St. Louis, MO) assay. Cells were seeded on a 96-well plate at a density of 1×10^4 and 5×10^2 cells/well for 24-hour and 5-day assay, respectively. For the MTT assay, transfected cells were allowed to proliferate for 5 days; cells were incubated with several concentrations (ranging from 1.25 to 10 μM) of MO-I-1151 and examined at various time points. After re-incubation for 1 hour with MTT solution, dimethyl sulfoxide (DMSO) was added to dissolve the resulting formazan crystals. The absorbance was measured in a microplate reader at a wavelength of 595 nm with a reference at 690-nm, and the results were expressed as a percent of absorbance relative to that of control.

Soft Agar Colony Formation Assay

Cells were suspended in complete medium containing 0.4% Noble agar (Sigma-Aldrich, St. Louis, MO, A5431) at the density of 2.5×10^3 cells/well and laid over a bottom agar mixture consisting of complete medium with 0.8% Noble agar on a 6-well plate. Cells were cultured for 3 weeks and treated twice a week in the absence or presence of different concentrations of MO-I-1151. Following this incubation period, formed colonies were stained with 10% giemsa solution and analyzed by Image J software (NIH, Bethesda, MD).

Senescence-associated β-galactosidase (SA-β-Gal) Staining

To detect senescent cells, a Detection Kit (K320-250, BioVision Inc, Milpitas, CA) was used, and the staining was performed according to manufacturer's instructions. Cultured cells were seeded onto a 12-well plate at a density of $5–10 \times 10^4$, $1.5–3 \times 10^5$ and 1×10^5 cells/well for FOCUS, Huh7 and HepG2 human HCC cell lines, respectively. After 24 hours of incubation, SA-β-Gal staining was performed.

To determine the effect of MO-I-1151, cells were exposed to DMSO or MO-I-1151 (5 μM) for 24 hours before staining. By counting the numbers of the blue-colored and total cells, the percent of cells that stained blue reflected the number of senescence-associated cells.

For murine models, tumor tissue samples were dissected and frozen in OCT compound. Seven micron sections were cut and SA-β-Gal staining was performed. For the quantification of senescence activity, 4 microscopic fields were randomly selected at high power magnification and the average number of blue-colored cells was determined.

Western Blot Analysis

The procedure and antibodies used for Western blot analysis are listed in the Supplementary Material.

In Vivo Study

Six-week-old female nu/nu nude mice (Charles River Laboratories, Wilmington, MA) were kept under pathogen-free conditions, fed standard food, and given free access to sterilized water. A subcutaneous xenograft model was used to analyze the dose-response efficacy of MO-I-1151 *in vivo*, as described previously. (7) Briefly, 1×10^7 FOCUS cells were inoculated into the right dorsal flank. On day 3 after inoculation, each concentration of MO-I-1151 (ranging from 0.1 to 10 mg/kg) prepared in DMSO was administered to mice by intraperitoneal injection on 5 consecutive days per week. Tumor size was measured using calipers twice per week, and tumor volumes were calculated as $A \times B^2 \times 0.5$ (A, length; B, width). An orthotopic xenograft model was created by direct intrahepatic inoculation of FOCUS human HCC cells, as described previously. (7) Briefly, 5×10^6 FOCUS cells suspended in 50 μl of serum free medium and 50 μl of Matrigel (Becton, Dickinson and Company, Franklin Lakes, NJ) were injected into the liver parenchyma. On day 3 after inoculation, MO-I-1151 (10 mg/kg) or DMSO was administered to mice by intraperitoneal injection on 5 consecutive days per week for 3 weeks. At the 4th week after initiation of treatment, mice were sacrificed to assess the anti-tumor effects of MO-I-1151. All procedures were approved by the institutional animal care and use committee of Rhode Island Hospital (Providence, RI).

Results

Knockdown or Knockout of ASPH Induces Cellular Senescence in Human HCC Cell Lines

ASPH expression is critically involved in HCC growth and progression. (12) FOCUS, Huh7 and HepG2 cells have high levels of ASPH protein as described previously. (7) To characterize the effects of manipulated ASPH levels on the HCC phenotype, we performed shRNA-mediated knockdown and CRISPR/Cas9-mediated knockout (18) of ASPH in those human HCC cell lines. A significant reduction of ASPH protein expression using shRNA-mediated knockdown of ASPH (shASPH) was demonstrated in FOCUS and Huh7 cells. CRISPR/Cas9-mediated knockout of ASPH (KO ASPH) was observed in HepG2 cells (Figure 1A). MTT assay demonstrated a significant reduction in cell proliferation following knockdown (shASPH) or knockout of ASPH (KO ASPH) compared with shRNA-luciferase (shLuc) or empty vector (EV) control, respectively (Figure 1A). Additionally, anchorage-

independent colony formation assays revealed that knockdown and knockout of ASPH significantly reduced (Figure 1B) colony formation in soft agar as one of reliable tests for assessing malignant stemness potential. (12) Cellular senescence was evaluated using SA-β-gal staining (Figure 1C). Transfection of the control construct (shLuc or EV) produced little blue staining. In contrast, knockdown or knockout of ASPH, caused substantial increase in β-gal staining as a marker for the cells undergoing senescence. Furthermore, senescence-associated secretory phenotypes (SASPs) (19, 20) were up-regulated (Supplementary Figure 1), and γH2AX (as the marker of DNA damage) and intracellular reactive oxygen species (ROS) levels tended to be induced (21) (Supplementary Figure 2 and 3); which are all associated with a senescent cell phenotype; following knockdown or knockout of ASPH expression compared with control.

The β-hydroxylase Inhibitor Induces Cellular Senescence in Human HCC Cell Lines

The SMIs were characterized using FOCUS cells in a 24-hour MTT assay. The results suggested that the biological activity of MO-I-1151 was more potent at lower concentrations than the 1st generation parent molecule MO-I-1100. Compared to several other SMIs, MO-I-1151 had the most robust anti-tumor effects on HCC cell proliferation (Figure 2A). To analyze the effects of this β-hydroxylase inhibitor on the HCC phenotype, MTT, anchorage-independent colony formation and SA-β-gal staining reaction of human HCC cell lines were performed. The MTT results revealed that MO-I-1151 significantly reduced cell proliferation in a dose-dependent manner over 5 days (Figure 2B). After 3-week exposure of MO-I-1151, anchorage-independent colony numbers were found to be significantly reduced in a dose-dependent manner (Figure 2C). The SA-β-gal staining revealed that senescent tumor cells were significantly induced by MO-I-1151 treatment compared with DMSO (Figure 2D). Taken together, these findings suggest that enzymatic inhibition of ASPH reduces human HCC cell proliferation through induction of cellular senescence.

Specificity of MO-I-1151 for ASPH β-hydroxylase activity

To analyze whether the anti-tumor effect of MO-I-1151 was specific to ASPH rather than other β-hydroxylases, we performed MTT and SA-β-gal staining reactions with shRNA-mediated knockdown and CRISPR/Cas9-mediated knockout of ASPH in the human HCC cell lines. MTT assays demonstrated significantly inhibitory effects of MO-I-1151 on cell proliferation at each concentration employed in human HCC cells with prior knockdown or knockout of ASPH compared with the control (shLuc or EV) after 24 hours (Figure 3A). As expected, the SMI exerted reduced but not complete inhibition of cell growth when ASPH expression was significantly altered to suggest that there might be ASPH independent effects as well. Additionally, MO-I-1151 treatment significantly induced the expression of SA-β-gal positive cells in the control (shLuc or EV) cells; in contrast, induction of cellular senescence was substantially blocked in response to knockdown or knockout of ASPH (Figure 3B). These findings imply that MO-I-1151 does not have biologic activity under conditions of reduced or absent ASPH expression in HCC. More importantly, these findings suggest that MO-I-1151 is a specific enzymatic inhibitor of ASPH.

ASPH Modulates Phosphorylation of GSK3β and Expression of Cell Cycle Regulators

The potential molecular pathways involved in cellular senescence induction were explored under conditions of ASPH knockdown (shASPH) and ASPH inhibition by MO-I-1151. We found a significant increase of phospho-GSK3β (inactivated form) with equal protein expression of GSK3β when comparing the shASPH to the shLuc control. Glycogen synthase (GS) expression increased whereas phospho-GS (p-GS) remained unchanged. Furthermore, p16, which is a cyclin-dependent kinase inhibitor, was increased, whereas cyclin D1 and PCNA levels were decreased (as cell proliferation markers) in response to shASPH (Figure 4A). In addition, GSK3β activity was inhibited after MO-I-1151 treatment similar to effects observed with knockdown of ASPH since phospho-GSK3β increased whereas total GSK3β protein levels did not change. Moreover, p16 increased whereas cyclin D1 and PCNA levels decreased in a dose-dependent manner (Figure 4B). Furthermore, SMI treatment increased p15 and p21 protein levels, as another senescence marker, in a dose dependent manner (Supplementary Figure 4). These findings indicate that changes in the levels of cell cycle regulators are important as potential mechanisms to induce senescence following inhibition of ASPH activity.

ASPH Modulates Cellular Senescence through GSK3β activity

To explore how ASPH modulates cellular senescence, we applied a constitutive active (CA)-GSK3β in Huh7 cells. The efficacy of transient transfection was evaluated using a plasmid encoding for green fluorescent protein (GFP). After a 48-hour transfection, < 5% of FOCUS (Supplementary Figure 5A) cells were positive; in contrast, > 95% of Huh7 cells were transfected (Supplementary Figure 5B), which was used for subsequent experiments. The MTT and anchorage-independent colony formation assays indicated that overexpression of CA-GSK3β induced proliferation significantly in ASPH knockdown (shASPH) cells, but not in the control (shLuc) cells (Figure 4C and 4D). SA-β-gal staining revealed that senescent HCC cells were significantly induced following knockdown of ASPH (shASPH). Moreover, this phenomenon was reversed by overexpression of CA-GSK3β as compared to no change in the control (shLuc) (Figure 4E). We also evaluated if overexpression of CA-GSK3β influences the expression of several key cell cycle regulators related to senescence. High level expression of GS was found only in knockdown of ASPH (shASPH); overexpression of CA-GSK3β significantly reduced GS; whereas phospho-GS levels remained unchanged. These findings supported the concept that GSK3β activity was inhibited in knockdown of ASPH and the subsequent phenotype could be reversed by overexpression of CA-GSK3β, compared to the shLuc transfected control. Furthermore, p16 was significantly decreased, but cyclin D1 and PCNA were increased following knockdown of ASPH in the context of overexpression of CA-GSK3β (Figure 4F). Taken together, these results suggest that inhibitory effects of ASPH on cellular senescence were mediated through GSK3β activity.

ASPH Directly Binds to GSK3β and Inhibits Its Phosphorylation by the Upstream Kinases

GSK3β is a serine/threonine kinase that has critical functions in numerous signaling pathways. Unlike most other protein kinases, GSK3β activity is inhibited by phosphorylation on serine (Ser9) by the actions of at least three pathways: 1) protein kinase B (AKT); 2) mitogen-activated protein kinases (MAPKs) including p38, extracellular signal-

regulated kinase (ERK) and c-Jun N-terminal kinase (JNK); and 3) ribosomal protein S6 kinase (S6K) signaling. (22) To determine which pathway is activated in response to knockdown of ASPH in human HCC cells, we evaluated the expression of the upstream kinases of GSK3β. However, AKT, p38, ERK, JNK and S6K levels were not changed following knockdown of ASPH (Supplementary Figure 6A). To investigate how phosphorylation of GSK3β is regulated, we used HEK293 cells co-transfected with GSK3β vs. ASPH to analyze the potential contribution of protein-protein interaction. Protein overexpression was confirmed in HEK293 cells after co-transfection with HA-tagged ASPH, wild type (WT)-GSK3β or empty vector (EV) plasmids (Figure 5A). Direct protein-protein interaction between GSK3β and ASPH was demonstrated by co-immunoprecipitation (IP). Immunoblotting with anti-GSK3β revealed that GSK3β bound to ASPH following co-transfection with WT-GSK3β and ASPH (Figure 5B). In addition, we used overexpression of ASPH only in HEK293 cells and confirmed that overexpressed ASPH and endogenous expressed GSK3β had a direct interaction after insulin treatment (Supplementary Figure 7). Previous studies have indicated that insulin treatment up-regulates ASPH expression. (23) Furthermore, we assessed protein-protein interactions between GSK3β and its upstream kinases by co-IP. In HEK293 cells, co-transfection of WT-GSK3β with either HA-tagged ASPH or EV (Figure 5C) revealed that the GSK3β upstream kinase protein levels (AKT, p38) were unchanged in co-transfected HEK293 cells when ASPH was overexpressed (Supplementary Figure 6B). Under these conditions, immunoblotting with antibodies against the upstream kinases of GSK3β, in immunopurified samples by anti-GSK3β, demonstrated that GSK3β was able to bind strongly to AKT and p38 (the binding to ERK, JNK and S6K were undetectable, data not shown) in the absence of ASPH. When ASPH was overexpressed, GSK3β bound to ASPH, rather than AKT or p38 (Figure 5D). These observations suggest that ASPH directly binds to GSK3β (through competing with AKT and p38) and thus inhibits the subsequent phosphorylation of GSK3β by its upstream kinases.

Anti-tumor Effects of MO-I-1151 on Subcutaneous and Intrahepatic Xenograft HCC Tumor Models

In order to evaluate the anti-tumor effects of MO-I-1151 on HCC growth and progression *in vivo*, we established subcutaneous and orthotopic xenograft models of HCC. (7) The compound MO-I-1151 was administered to mice bearing FOCUS-generated tumors. On a subcutaneous xenograft model, mean tumor volume in the MO-I-1151 treated group was significantly reduced in a dose-dependent manner at the concentration ranging from 0.5 to 10 mg/kg compared to DMSO treated control (Figure 6A). On an orthotopic xenograft model, animals were sacrificed at 4 weeks and HCC intrahepatic growth was measured. Mean tumor weight in the MO-I-1151 treated group was significantly reduced compared to DMSO treated control (Figure 6B). A significant increase in the phospho-GSK3β/GSK3β ratio and p16 expression was observed in tumor lysates derived from the MO-I-1151 treated animals when compared to DMSO treated controls (Figure 6C). Furthermore, SA-β-gal staining illustrated a significant induction of cellular senescence in MO-I-1151 treated animals compared to the DMSO treated controls (Figure 6D). These findings suggest that this 2nd generation SMI of β-hydroxylase activity reduces HCC growth in a dose-dependent manner and promotes senescence *in vivo*.

Discussion

ASPH is highly upregulated in HCC tumors, (6, 7, 24, 25) and lacks expression in dysplastic regenerating nodules, suggesting its role in hepatic oncogenesis. (7) Some of the biological functions of ASPH has been determined. Its overexpression promotes cell proliferation, anchorage-independent colony formation, motility, migration, invasion and metastasis, which are characteristics of the malignant phenotype. (7–9, 12) ASPH has been shown to directly interact with Notch1 and JAG1 to activate Notch signaling in HCC cell lines. (25, 26) We have recently developed a first generation β-hydroxylase inhibitor and clarified that the biological function of ASPH requires enzymatic activity. (7, 8) However, ASPH has the potential to modify function of numerous proteins that have calcium dependent EGF-like repeats by catalyzing the hydroxylation of aspartyl and asparaginyl residues that may also contribute to the development of malignancy.

GSK3β is a multifunctional serine/threonine kinase that participates in numerous signaling pathways involved in various physiological processes. GSK3β was initially described as a key enzyme involved in glycogen metabolism (27); currently it is known to regulate diverse functions, including cell division, apoptosis, microtubule interactions and cell fate determination during embryonic development. (22) Dysregulation of GSK3β has been implicated in various human diseases including cancer. (28) In this context, GSK3β had not previously been considered to be a therapeutic target during tumorigenesis since inhibitors may enhance aberrant canonical WNT/β-catenin signaling cascade, which is activated in a variety of human tumors including HCC. (29, 30) Recent studies suggest, however, that several types of tumors may be susceptible to GSK3β inhibitors, leading to significant reduction in cell proliferation. (31–33)

The functional relationships of GSK3β with its target genes are cell context dependent. For instance, inhibition of GSK3β promotes the dephosphorylation and stabilization of cyclin D1 in non-tumor cells (34); conversely, it decreases cyclin D1 expression in several types of tumor cells (33, 35). In this study, we demonstrated that p16 was induced, while cyclin D1 and PCNA were reduced following phosphorylation of GSK3β in human HCC cell lines. This phenomenon was related to the expression level of ASPH as shown by shRNA-mediated knockdown of this enzyme; enzymatic function was deemed to be important as shown by treatment of HCC cells with a SMI of β-hydroxylase activity. In addition, we determined that overexpression of a constitutive active GSK3β reversed p16, cyclin D1 and PCNA expression patterns under knockdown conditions of ASPH in human HCC cell lines. These results support the notion that changes of p16, cyclin D1 and PCNA, as modulated by ASPH expression levels are likely to be transmitted through the GSK3β signaling cascade.

GSK3β is active in resting cells and functionally inactivated after phosphorylation by various kinases in response to different cellular stimuli. Three different signaling pathways are known to inactivate GSK3β; AKT, MAPKs and S6K. (22) We evaluated the total and phosphorylated forms of AKT, p38/ERK/JNK and S6K following knockdown of ASPH to determine which pathway is activated. Surprisingly, none of these pathways was altered. Furthermore, we demonstrated that ASPH expression remained the same following overexpression of a constitutive active GSK3β. Thus aberrant expression of ASPH in HCC

cells was not regulated by GSK3β activity. Taken together, we hypothesized that there exist other functional interactions between ASPH and GSK3β, which contribute to the generation of a malignant phenotype; and thus, we focused on protein-protein interactions between GSK3β, ASPH and its upstream kinases. Interestingly, GSK3β physically bound to ASPH. More important, this event led to reduced GSK3β-binding to AKT and p38 (upstream kinases), and was directly influenced by the level of ASPH in cells. Therefore, phosphorylation of GSK3β was blocked from its upstream kinases due to a physical interaction with ASPH.

Recently, Favaro E, et al. demonstrated that inhibition of glycogen mobilization in cancer cells leads to induction of senescence and impairs tumor growth. (36) Furthermore, inhibitors of GSK3β have been shown to induce cellular senescence; which was accompanied by enhanced glycogenesis and increased glycogen content. (37) In this study, we did not observe a consistent change in the amount of glycogen storage by using Periodic acid-Schiff staining (data not shown). However, changes in glycogen synthase activity was observed along with induction of cellular senescence through phosphorylation of GSK3β.

Characteristics of senescent cells are growth arrest and altered gene expression, including changes in cell-cycle inhibitors or activators. (14) Several markers can robustly identify senescent cells; SA-β-gal is the most accepted and widely used cellular marker. (38) Cellular senescence is triggered by a combination of at least three mechanisms: telomere shortening, upregulation of the cyclin-dependent kinase inhibitor 2A (CDKN2A) locus (which encodes $p16^{INK4A}$ and $p14^{ARF}$), and accumulation of DNA damage. (39) Recent studies have disclosed a close correlation of senescence with pre-malignant stages of tumorigenesis (40), but in the fully transformed malignant phenotype, this regulatory mechanism is lost. (40) Accumulating evidence supports a key role for cellular senescence as a barrier to tumor progression. Indeed, cellular senescence is prevalent in pre-malignant lesions, and progression to neoplasia requires evading this regulatory process. A class of tumor suppressors (for example $p16^{INK4A}$ and $p14^{ARF}$) monitors stress signals, and the activation of these signals triggers cellular senescence. Their loss or inactivation may confer impaired cellular senescence, unleashing malignant growth and progression. (41) In this study, we demonstrated that SA-β-gal and p16 expression were induced through phosphorylation of GSK3β in human HCC cell lines, by using shRNA-mediated knockdown of ASPH as well as treatment with a β-hydroxylase inhibitor *in vitro*. We also demonstrated that a small molecule β-hydroxylase inhibitor strongly induced p15 and p21 expression levels, as other markers of cellular senescence. (14) In addition, we found that several markers associated with the senescent cell phenotype, including SASPs (19, 20), γH2AX and intracellular ROS levels (21), were up-regulated or induced after knockdown or knockout of ASPH expression in human HCC cell lines. Furthermore, overexpression of constitutive active GSK3β reversed SA-β-gal and p16 changes when ASPH cellular level was reduced. Consistently, when GSK3β activity was reduced, p16 expression and SA-β-gal activity was enhanced, particularly after using a β-hydroxylase inhibitor treatment of HCC tumor bearing mice. Mai W, et al. demonstrated that inhibition of GSK3β attenuated telomerase activity and increased SA-β-gal-positive cells in colon cancer cell lines. (33) Usually the senescent cells have

shortened telomere and decreased telomerase activity; thus, this report also supports the finding that cellular senescence is mediated through phosphorylation of GSK3β.

Tumorigenesis as a multistep process involves bypassing or inhibiting crucial mediators of cellular senescence, but this phenomenon does not necessarily imply that malignant cells have completely lost their capacity to undergo cellular senescence. (42) Recently, anti-tumor efficacy was shown by restoring the tumor suppressive function of p53 using murine models. (43) Moreover, tumor regression induced by cellular senescence was revealed to be accompanied by the presence of tumor-infiltrating neutrophils, macrophages and natural killer cells. (43) Recently, evidence has been presented that senescent cells can be eliminated through a SASP-mediated immune response (44), and we observed that SASPs were up-regulated after inhibition of ASPH in human HCC cell lines. So senescent tumor cells may be eliminated by the immune system, resulting in tumor regression. Therefore, senescence-inducing interventions could be a key platform for anti-tumor therapy. Senescence-inducing agents like MO-I-1151, by attacking tumor cells directly may prove to be effective alone or in combination with other therapeutic interventions. (42)

In conclusion, we have identified that shRNA-mediated knockdown and CRISPR/Cas9-mediated knockout of ASPH as well as enzymatic inhibition of ASPH guide human HCC cells to undergo cellular senescence. Inhibition of ASPH activity induces senescence as mediated through phosphorylation of GSK3β. In addition, ASPH binding to GSK3β inhibits its phosphorylation (inactivation) and thus blocks the signal transduction from its upstream kinases as shown by the proposed model presented in Figure 7. Our findings suggest that ASPH can be a potential therapeutic target and a 2nd generation β-hydroxylase inhibitor is an effective anti-tumor agent against intrahepatic HCC growth and progression partially through the induction of cellular senescence.

Supplementary Material

Refer to Web version on PubMed Central for supplementary material.

Acknowledgements

The authors gratefully acknowledge the assistance of Lelia C. Noble in the preparation of the sections from OCT frozen samples.

Grant Support: This project was supported by NIH grants CA123544 and AA20587.

Abbreviations

AKT	protein kinase B
ASPH	aspartate β-hydroxylase
CA	constitutive active
CCC	cholangiocellular carcinoma
CPT	camptothecin

CXCL	chemokine (C-X-C motif) ligand
DAPI	4’,6-diamidino-2-phenylindole
DMSO	dimethyl sulfoxide
EGF	epidermal growth factor
ERK	extracellular signal-regulated kinase
EV	empty vector
GAPDH	glyceraldehyde 3-phosphate dehydrogenase
GFP	green fluorescent protein
GS	glycogen synthase
GSK3β	glycogen synthase kinase 3β
HBV	hepatitis B virus
HCC	hepatocellular carcinoma
IL	interleukin
IP	immunoprecipitation
JNK	c-Jun N-terminal kinase
KO	knockout
MAPK	mitogen-activated protein kinase
MTT	3-(4,5-dimethylthiazol-2-yl)-2,5-diphenyl-tetrazolium bromide
ROS	reactive oxygen species
SA-β-gal	senescence-associated β-galactosidase
SASP	senescence-associated secretory phenotype
S.D.	standard deviation
S.E.M.	standard error of the mean
SMI	small molecule inhibitor
S6K	ribosomal protein S6 kinase
WT	wild type

References

1. Parkin DM. Global cancer statistics in the year 2000. Lancet Oncol. 2001; 2:533–543. [PubMed: 11905707]
2. El-Serag HB. Hepatocellular carcinoma. N Engl J Med. 2011; 365:1118–1127. [PubMed: 21992124]
3. Villanueva A, Hernandez-Gea V, Llovet JM. Medical therapies for hepatocellular carcinoma: a critical view of the evidence. Nat Rev Gastroenterol Hepatol. 2013; 10:34–42. [PubMed: 23147664]

4. Jia S, VanDusen WJ, Diehl RE, Kohl NE, Dixon RA, Elliston KO, Stern AM, et al. cDNA cloning and expression of bovine aspartyl (asparaginyl) beta-hydroxylase. J Biol Chem. 1992; 267:14322–14327. [PubMed: 1378441]
5. Engel J. EGF-like domains in extracellular matrix proteins: localized signals for growth and differentiation? FEBS Lett. 1989; 251:1–7. [PubMed: 2666164]
6. Lavaissiere L, Jia S, Nishiyama M, de la Monte S, Stern AM, Wands JR, Friedman PA. Overexpression of human aspartyl(asparaginyl)beta-hydroxylase in hepatocellular carcinoma and cholangiocarcinoma. J Clin Invest. 1996; 98:1313–1323. [PubMed: 8823296]
7. Aihara A, Huang CK, Olsen MJ, Lin Q, Chung W, Tang Q, Dong X, et al. A cell-surface beta-hydroxylase is a biomarker and therapeutic target for hepatocellular carcinoma. Hepatology. 2014; 60:1302–1313. [PubMed: 24954865]
8. Dong X, Lin Q, Aihara A, Li Y, Huang CK, Chung W, Tang Q, et al. Aspartate beta-Hydroxylase expression promotes a malignant pancreatic cellular phenotype. Oncotarget. 2015; 6:1231–1248. [PubMed: 25483102]
9. Sepe PS, Lahousse SA, Gemelli B, Chang H, Maeda T, Wands JR, de la Monte SM. Role of the aspartyl-asparaginyl-beta-hydroxylase gene in neuroblastoma cell motility. Lab Invest. 2002; 82:881–891. [PubMed: 12118090]
10. Luu M, Sabo E, de la Monte SM, Greaves W, Wang J, Tavares R, Simao L, et al. Prognostic value of aspartyl (asparaginyl)-beta-hydroxylase/humbug expression in non-small cell lung carcinoma. Hum Pathol. 2009; 40:639–644. [PubMed: 19200576]
11. Wang J, de la Monte SM, Sabo E, Kethu S, Tavares R, Branda M, Simao L, et al. Prognostic value of humbug gene overexpression in stage II colon cancer. Hum Pathol. 2007; 38:17–25. [PubMed: 17020779]
12. Ince N, de la Monte SM, Wands JR. Overexpression of human aspartyl (asparaginyl) beta-hydroxylase is associated with malignant transformation. Cancer Res. 2000; 60:1261–1266. [PubMed: 10728685]
13. Hayflick L. THE LIMITED IN VITRO LIFETIME OF HUMAN DIPLOID CELL STRAINS. Exp Cell Res. 1965; 37:614–636. [PubMed: 14315085]
14. Campisi J, d'Adda di Fagagna F. Cellular senescence: when bad things happen to good cells. Nat Rev Mol Cell Biol. 2007; 8:729–740. [PubMed: 17667954]
15. Hanahan D, Weinberg RA. The hallmarks of cancer. Cell. 2000; 100:57–70. [PubMed: 10647931]
16. Campisi J. Cellular senescence as a tumor-suppressor mechanism. Trends Cell Biol. 2001; 11:S27–S31. [PubMed: 11684439]
17. Dimri GP. What has senescence got to do with cancer? Cancer Cell. 2005; 7:505–512. [PubMed: 15950900]
18. Wiedenheft B, Sternberg SH, Doudna JA. RNA-guided genetic silencing systems in bacteria and archaea. Nature. 2012; 482:331–338. [PubMed: 22337052]
19. Coppe JP, Patil CK, Rodier F, Sun Y, Munoz DP, Goldstein J, Nelson PS, et al. Senescence-associated secretory phenotypes reveal cell-nonautonomous functions of oncogenic RAS and the p53 tumor suppressor. PLoS Biol. 2008; 6:2853–2868. [PubMed: 19053174]
20. Coppe JP, Desprez PY, Krtolica A, Campisi J. The senescence-associated secretory phenotype: the dark side of tumor suppression. Annu Rev Pathol. 2010; 5:99–118. [PubMed: 20078217]
21. Kuilman T, Michaloglou C, Mooi WJ, Peeper DS. The essence of senescence. Genes Dev. 2010; 24:2463–2479. [PubMed: 21078816]
22. Cohen P, Frame S. The renaissance of GSK3. Nat Rev Mol Cell Biol. 2001; 2:769–776. [PubMed: 11584304]
23. de la Monte SM, Tamaki S, Cantarini MC, Ince N, Wiedmann M, Carter JJ, Lahousse SA, et al. Aspartyl-(asparaginyl)-beta-hydroxylase regulates hepatocellular carcinoma invasiveness. J Hepatol. 2006; 44:971–983. [PubMed: 16564107]
24. Wang K, Liu J, Yan ZL, Li J, Shi LH, Cong WM, Xia Y, et al. Overexpression of aspartyl-(asparaginyl)-beta-hydroxylase in hepatocellular carcinoma is associated with worse surgical outcome. Hepatology. 2010; 52:164–173. [PubMed: 20578260]
25. Cantarini MC, de la Monte SM, Pang M, Tong M, D'Errico A, Trevisani F, Wands JR. Aspartyl-asparagyl beta hydroxylase over-expression in human hepatoma is linked to activation of insulin-

like growth factor and notch signaling mechanisms. Hepatology. 2006; 44:446–457. [PubMed: 16871543]

26. Gundogan F, Bedoya A, Gilligan J, Lau E, Mark P, De Paepe ME, de la Monte SM. siRNA inhibition of aspartyl-asparaginyl beta-hydroxylase expression impairs cell motility, Notch signaling, and fetal growth. Pathol Res Pract. 2011; 207:545–553. [PubMed: 21862239]
27. Embi N, Rylatt DB, Cohen P. Glycogen synthase kinase-3 from rabbit skeletal muscle. Separation from cyclic-AMP-dependent protein kinase and phosphorylase kinase. Eur J Biochem. 1980; 107:519–527. [PubMed: 6249596]
28. Martinez A. Preclinical efficacy on GSK-3 inhibitors: towards a future generation of powerful drugs. Med Res Rev. 2008; 28:773–796. [PubMed: 18271054]
29. Anastas JN, Moon RT. WNT signalling pathways as therapeutic targets in cancer. Nat Rev Cancer. 2013; 13:11–26. [PubMed: 23258168]
30. Wands JR, Kim M. WNT/beta-catenin signaling and hepatocellular carcinoma. Hepatology. 2014; 60:452–454. [PubMed: 24644061]
31. Wang Z, Smith KS, Murphy M, Piloto O, Somervaille TC, Cleary ML. Glycogen synthase kinase 3 in MLL leukaemia maintenance and targeted therapy. Nature. 2008; 455:1205–1209. [PubMed: 18806775]
32. Chen EY, DeRan MT, Ignatius MS, Grandinetti KB, Clagg R, McCarthy KM, Lobbardi RM, et al. Glycogen synthase kinase 3 inhibitors induce the canonical WNT/beta-catenin pathway to suppress growth and self-renewal in embryonal rhabdomyosarcoma. Proc Natl Acad Sci U S A. 2014; 111:5349–5354. [PubMed: 24706870]
33. Mai W, Kawakami K, Shakoori A, Kyo S, Miyashita K, Yokoi K, Jin M, et al. Deregulated GSK3{beta} sustains gastrointestinal cancer cells survival by modulating human telomerase reverse transcriptase and telomerase. Clin Cancer Res. 2009; 15:6810–6819. [PubMed: 19903789]
34. Diehl JA, Cheng M, Roussel MF, Sherr CJ. Glycogen synthase kinase-3beta regulates cyclin D1 proteolysis and subcellular localization. Genes Dev. 1998; 12:3499–3511. [PubMed: 9832503]
35. Cao Q, Lu X, Feng YJ. Glycogen synthase kinase-3beta positively regulates the proliferation of human ovarian cancer cells. Cell Res. 2006; 16:671–677. [PubMed: 16788573]
36. Favaro E, Bensaad K, Chong MG, Tennant DA, Ferguson DJ, Snell C, Steers G, et al. Glucose utilization via glycogen phosphorylase sustains proliferation and prevents premature senescence in cancer cells. Cell Metab. 2012; 16:751–764. [PubMed: 23177934]
37. Seo YH, Jung HJ, Shin HT, Kim YM, Yim H, Chung HY, Lim IK, et al. Enhanced glycogenesis is involved in cellular senescence via GSK3/GS modulation. Aging Cell. 2008; 7:894–907. [PubMed: 18782348]
38. Dimri GP, Lee X, Basile G, Acosta M, Scott G, Roskelley C, Medrano EE, et al. A biomarker that identifies senescent human cells in culture and in aging skin in vivo. Proc Natl Acad Sci U S A. 1995; 92:9363–9367. [PubMed: 7568133]
39. Collado M, Blasco MA, Serrano M. Cellular senescence in cancer and aging. Cell. 2007; 130:223–233. [PubMed: 17662938]
40. Collado M, Gil J, Efeyan A, Guerra C, Schuhmacher AJ, Barradas M, Benguria A, et al. Tumour biology: senescence in premalignant tumours. Nature. 2005; 436:642. [PubMed: 16079833]
41. Sarkisian CJ, Keister BA, Stairs DB, Boxer RB, Moody SE, Chodosh LA. Dose-dependent oncogene-induced senescence in vivo and its evasion during mammary tumorigenesis. Nat Cell Biol. 2007; 9:493–505. [PubMed: 17450133]
42. Collado M, Serrano M. Senescence in tumours: evidence from mice and humans. Nat Rev Cancer. 2010; 10:51–57. [PubMed: 20029423]
43. Xue W, Zender L, Miething C, Dickins RA, Hernando E, Krizhanovsky V, Cordon-Cardo C, et al. Senescence and tumour clearance is triggered by p53 restoration in murine liver carcinomas. Nature. 2007; 445:656–660. [PubMed: 17251933]
44. Perez-Mancera PA, Young AR, Narita M. Inside and out: the activities of senescence in cancer. Nat Rev Cancer. 2014; 14:547–558. [PubMed: 25030953]

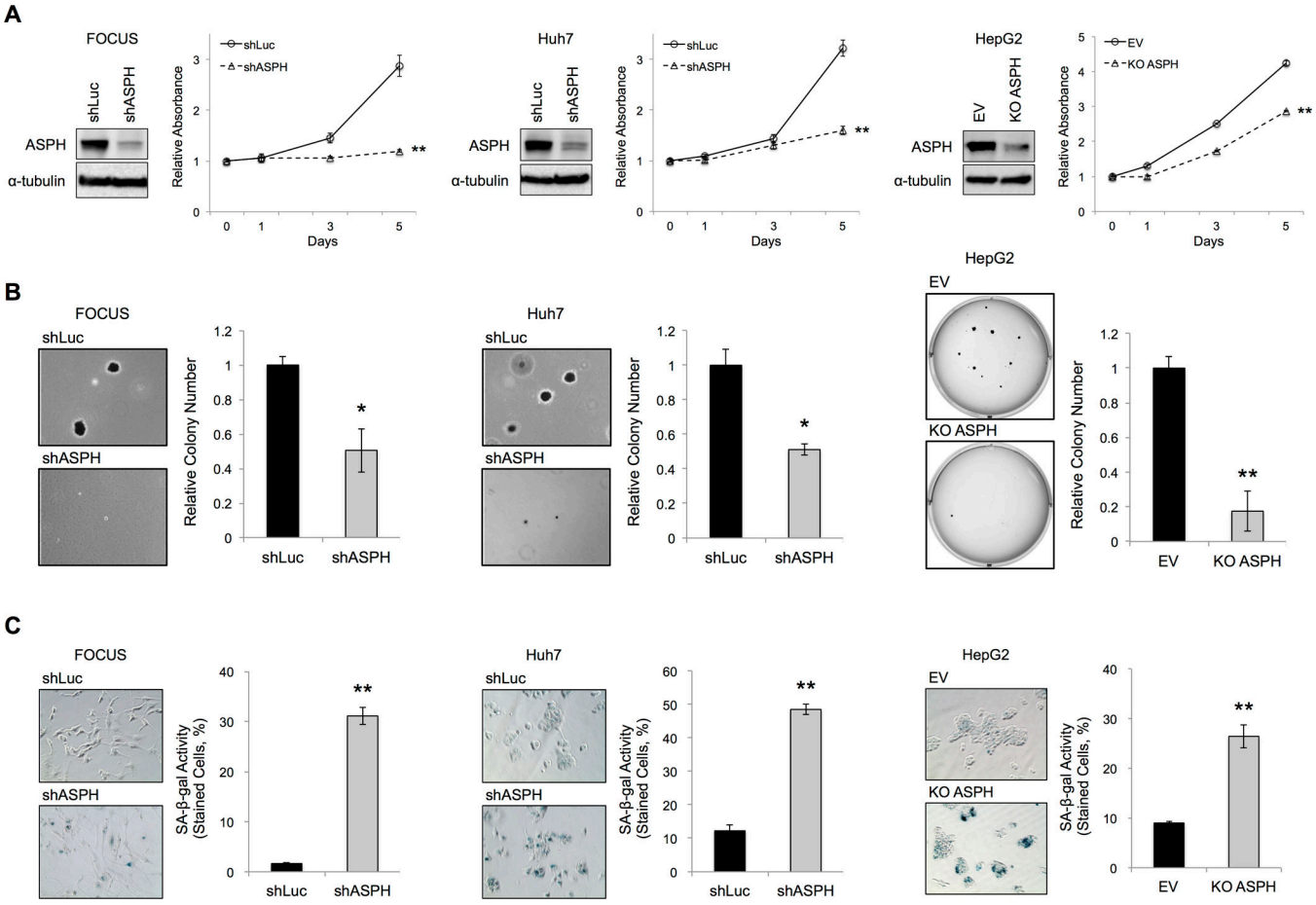

Figure 1. Effects of knockdown and knockout of ASPH on cell proliferation, anchorage-independent colony formation and cellular senescence in human HCC cell lines

The following assays were performed in human HCC cell lines expressing the control (shLuc) vs. knockdown of ASPH (shASPH) (FOCUS and Huh7), as well as control (EV) vs. knockout of ASPH (KO ASPH) (HepG2). **(A)** Protein expressions of ASPH in human HCC cell lines with knockdown (shASPH) or knockout of ASPH (KO ASPH) compared to the control (shLuc or EV). MTT assays showed relative absorbance at each time point over 5 days. **(B)** Representative photographs of anchorage-independent colony formation (left panel, 100×). The bar graphs indicated relative colony number (right panel). **(C)** Representative photographs of SA-β-gal staining (left panel, 200×). Senescent cells exhibited blue staining. Senescence under each condition was quantified and expressed as percent of SA-β-gal-positive cells (right panels). Mean ± S.D. of triplicate independent experiments. **P* < 0.05, ***P* < 0.01 compared to the control cells (shLuc or EV).

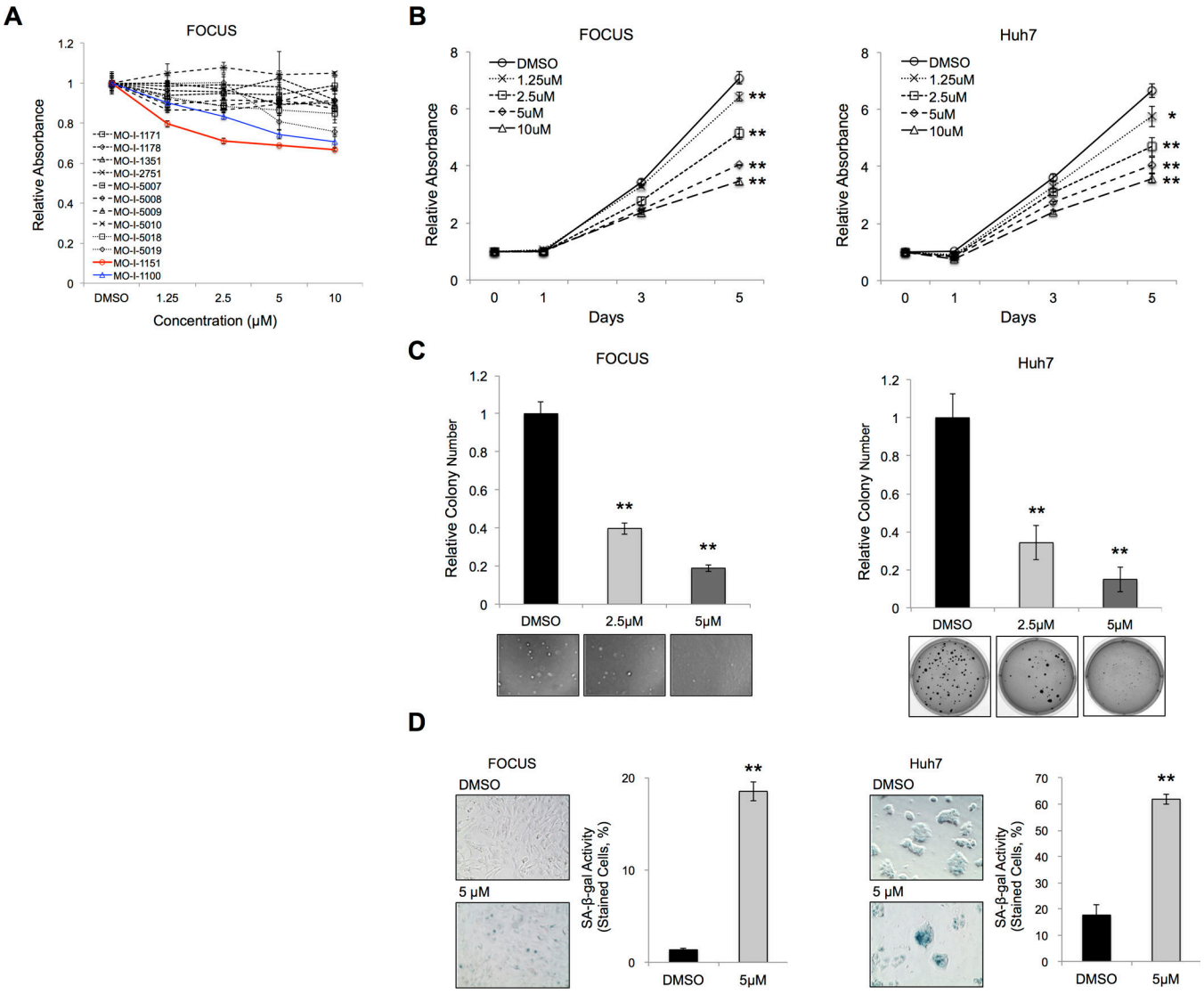

Figure 2. Characterization and Evaluation of anti-tumor effects of a SMI of β-hydroxylase (MO-I-1151) on the HCC phenotype

(A) MTT assays showed relative absorbance at each concentration (ranging from 1.25 to 10 μM) of MO-I-1151, MO-I-1100 and other candidate β-hydroxylase inhibitors (MO-I-1171, 1178, 1351, 2751, 5007, 5008, 5009, 5010, 5018 and 5019) which had no biologic activity. The assay was performed after 24-hour's exposure to DMSO or SMIs in FOCUS HCC cells. [Blue line was MO-I-1000 (the first generation SMI). red line was MO-I-1151 (the second generation SMI). Black lines represented other compounds that had no effect.] **(B)** MTT assays showed relative absorbance at each time point exposed to DMSO or different concentrations of MO-I-1151 (from 1.25 to 10 μM) for 5 days. **(C)** The bar graphs indicated relative colony numbers after 3-week exposure to DMSO or MO-I-1151 (2.5 or 5 μM). Representative photographs of anchorage-independent colony formation were shown. **(D)** Representative photographs of SA-β-gal staining after 24-hour's exposure to DMSO or MO-I-1151 (5 μM) (left panel, 200×). The SA-β-gal activity was quantified and expressed as

percent of SA-β-gal-positive cells (right panel). Mean ± S.D. of triplicate independent experiments. *$P < 0.05$, **$P < 0.01$ compared to DMSO treated cells.

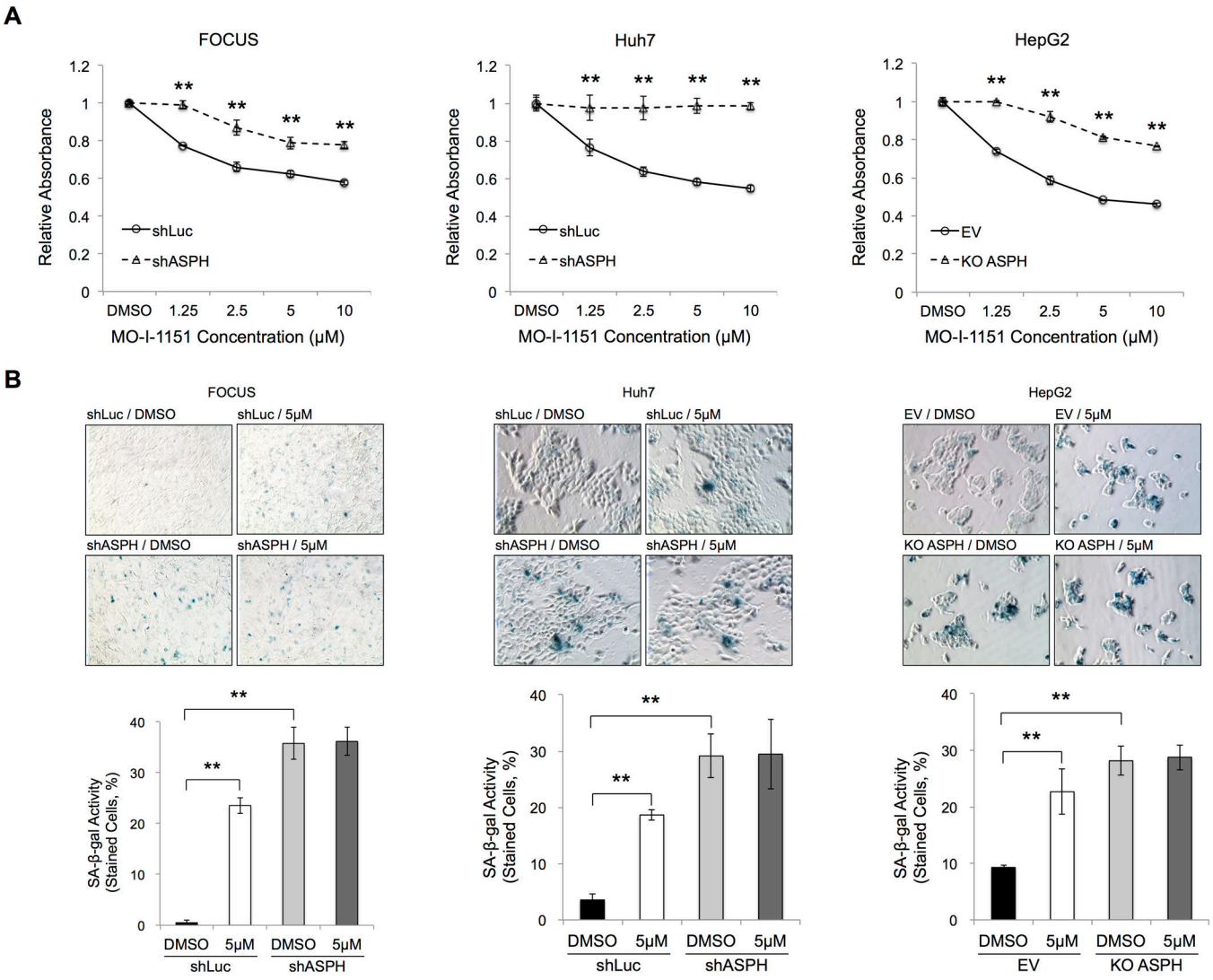

Figure 3. The β-hydroxylase inhibitor MO-I-1151 was specific for ASPH mediated biologic activity

The following assays were performed in human HCC cell lines stably expressing the control (shLuc) vs. knockdown of ASPH (shASPH) (FOCUS and Huh7), as well as the control (EV) vs. knockout of ASPH (KO ASPH) (HepG2). **(A)** MTT assays showed relative absorbance after 24-hour exposure to each concentration (ranging from 1.25 to 10 μM) of MO-I-1151 or DMSO. **(B)** SA-β-gal staining was performed after 24-hour exposure to DMSO or MO-I-1151 (5 μM). Representative photographs of SA-β-gal staining (top, 200×). Senescence under each condition was quantified and expressed as percentage of SA-β-gal-positive cells (bottom). Mean ± S.D. of triplicate independent experiments. $^{**}P < 0.01$ compared to the control cells (shLuc or EV) **(A)** or DMSO treated control cells (shLuc or EV) **(B)**.

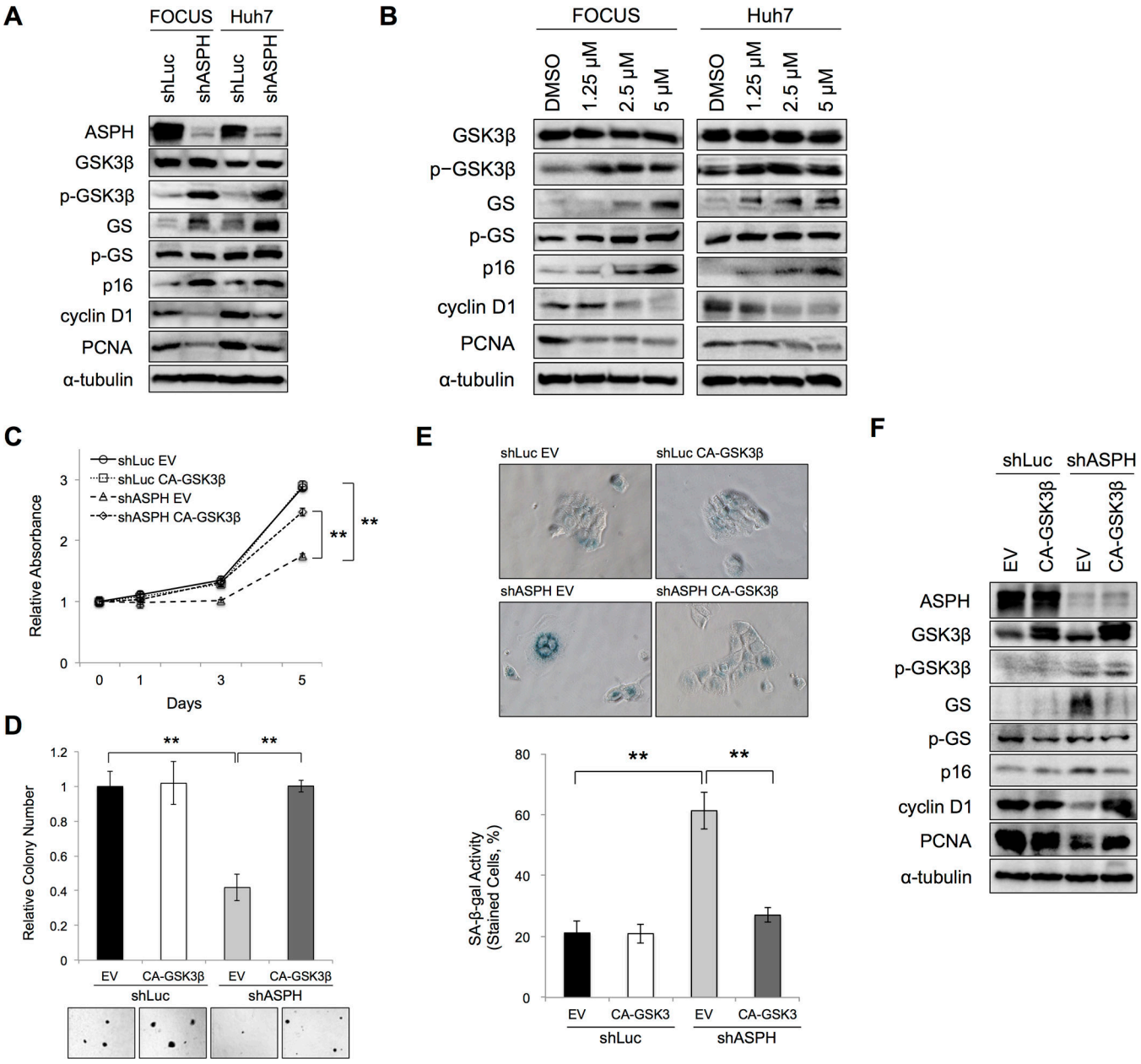

Figure 4. ASPH-related cellular senescence was mediated through GSK3β in human HCC cells

(A, B) Protein expressions of ASPH, GSK3β, phosho-GSK3β, GS, phospho-GS, p16, cyclin D1 and PCNA were evaluated by Western blot analysis. **(A)** In the control (shLuc) or knockdown of ASPH (shASPH) human HCC cell lines (FOCUS and Huh7). **(B)** After 24-hour exposure to DMSO or different concentrations of MO-I-1151 (from 1.25 to 5 μM) in human HCC cell lines (FOCUS and Huh7). **(C– F)** The following assays were performed in the control (shLuc) or knockdown of ASPH (shASPH) in Huh7 cells with or without overexpression of CA-GSK3β. **(C)** MTT assay showed relative absorbance at each time point over 5 days. **(D)** The bar graphs represented relative colony numbers (top). Representative photographs of anchorage-independent colony formation are shown (bottom, 100×). **(E)** Representative photographs of SA-β-gal staining (top, 200×). SA-β-gal activity

was quantified and expressed as percent of SA-β-gal-positive cells (bottom). **(F)** Protein expression of ASPH, GSK3β, phosho-GSK3β, GS, phospho-GS, p16, cyclin D1 and PCNA were evaluated by Western blot after 48-hour of co-transfection in Huh7 cells. Mean ± S.D. of triplicate independent experiments. $^{**}P < 0.01$ compared to shLuc + EV or shASPH + EV cells.

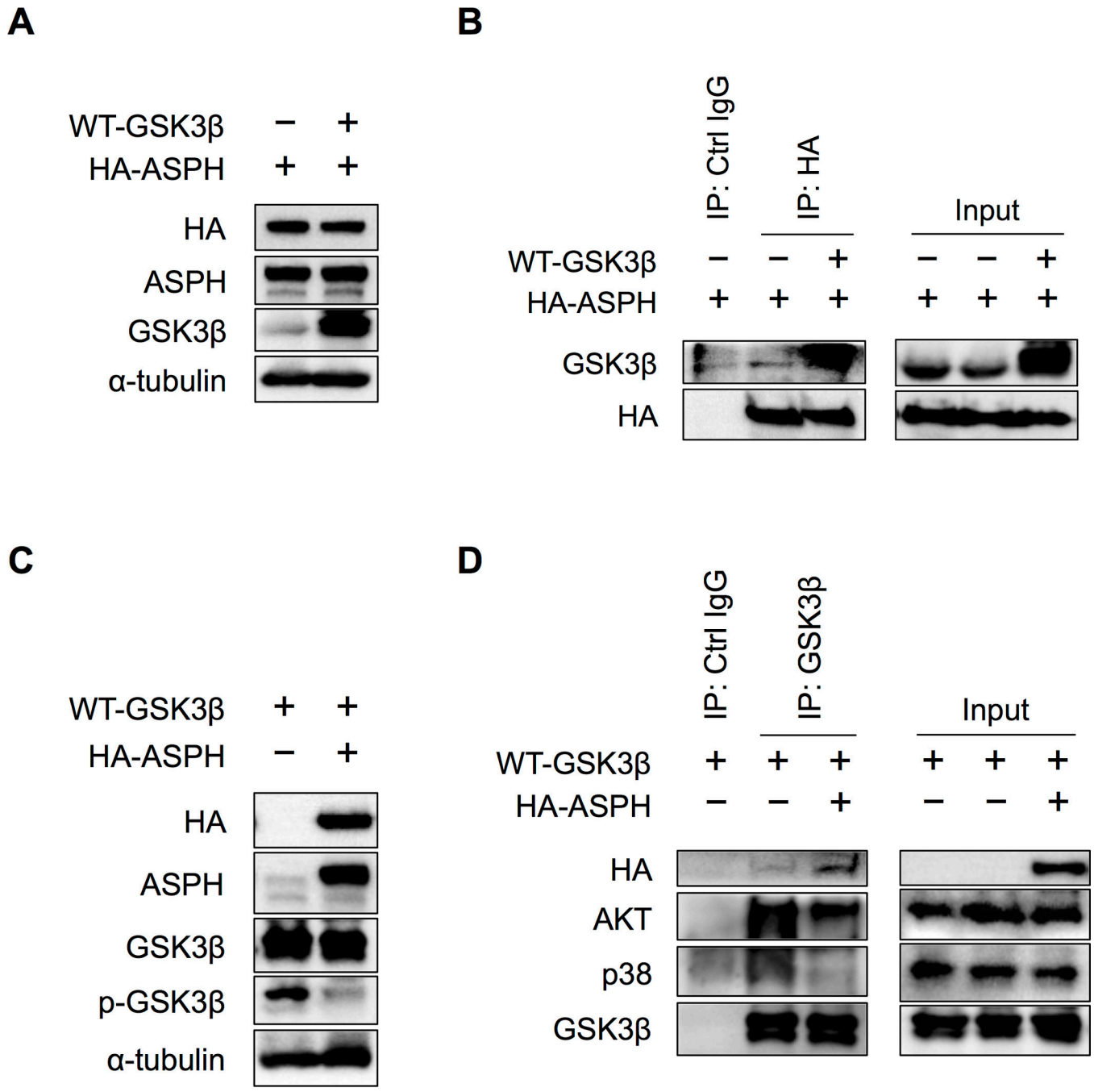

Figure 5. ASPH inhibited phosphorylation of GSK3β from its upstream kinases by directly binding to GSK3β

The following assays were performed in HEK293 cells after 48-hour co-transfection of **(A, B)** HA-tagged ASPH with either WT-GSK3β or EV plasmids; as well as **(C, D)** WT-GSK3β with either HA-tagged ASPH or EV plasmids. **(A)** Protein expressions of HA, ASPH and GSK3β were confirmed by Western blot analysis, in co-transfected HEK293 cells with HA-tagged ASPH and either WT-GSK3β or EV. Antibody against α-tubulin was used as a loading control. **(B)** After co-immunoprecipitation using control IgG or HA-probe, immunoblotting with HA-probe and antibody against GSK3β were performed. **(C)** Protein

expressions of HA, ASPH, GSK3β and phospho-GSK3β were confirmed by Western blot analysis, in co-transfected HEK293 cells with WT-GSK3β and either HA-tagged ASPH or EV. Antibody against α-tubulin was used as a loading control. **(D)** After co-immunoprecipitation using control IgG or anti-GSK3β antibody, immunoblotting with HA-probe and antibodies against AKT, p38 and GSK3β are shown.

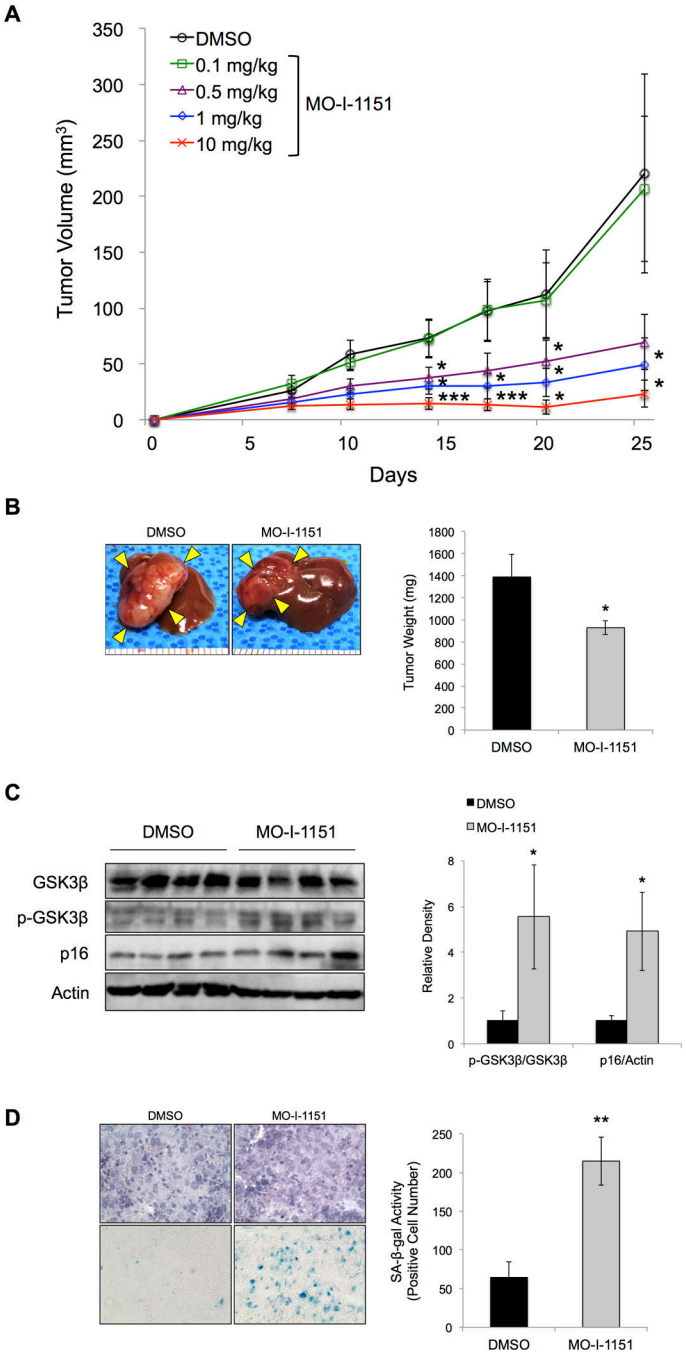

Figure 6. Anti-tumor effects of targeting ASPH in subcutaneous and orthotopic xenograft models generated by FOCUS HCC cells

(A) Mean tumor volume was measured and plotted twice per week in each concentration of MO-I-1151 treatment (ranging from 0.1 to 10 mg/kg), compared to DMSO (n = 8). **(B)** Representative photographs of intrahepatic inoculated tumors 4 weeks after initiation of MO-I-1151 treatment, compared to DMSO as control (left panel). Mean tumor weight was analyzed at 4 weeks after initiation of MO-I-1151 treatment, compared to DMSO (n = 5) (right panel). **(C)** Protein expression of GSK3β, phospho-GSK3β and p16 in tumor lysates

treated with MO-I-1151, compared to DMSO, was evaluated by Western blot (left panel). Ratio of the relative density of p-GSK3β/GSK3β or p16/Actin ratio (right panel). **(D)** Representative photographs of hematoxylin and eosin staining (top) and SA-β-gal staining (bottom) performed in serial sections of frozen tumor tissue samples treated with MO-I-1151, compared to DMSO (left panel, 400×). Senescence in the tumor sample was quantified and expressed as average number of SA-β-gal-positive cells (right panel). Mean ± S.E.M. *$P < 0.05$, **$P < 0.01$, ***$P < 0.005$ compared to the DMSO treated group.

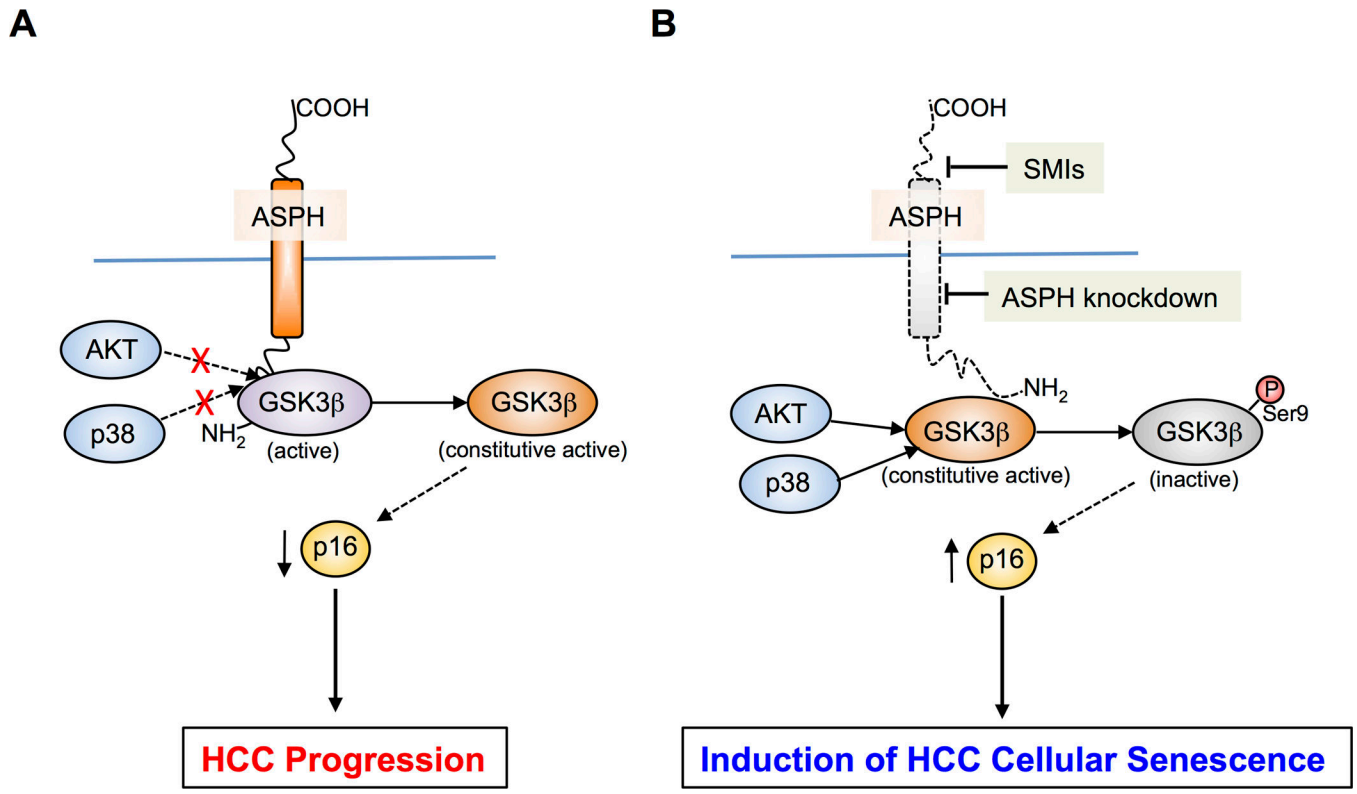

Figure 7. Hypothesis of how ASPH may mediate senescence of HCC cells

(A) ASPH overexpression is followed by binding to GSK3β (purple) and inhibits the interaction and subsequent phosphorylation of GSK3β by AKT and p38 upstream kinases (blue). This mechanism keeps GSK3β constitutive active (orange) and leads HCC progression by promoting degradation of the cyclin-dependent kinase inhibitor p16 (yellow). **(B)** Under conditions of Inhibition such as ASPH knockdown or modulation of enzymatic activity by SMIs (MO-I-1151), AKT and p38 upstream kinases can now phosphorylate and inactivate GSK3β function (gray). The net results are stabilization of p16, and promotion of HCC cell senescence.